Microfluidic platform for photodynamic therapy cytotoxicity analysis of nanoencapsulated indocyanine-type photosensitizers

Elżbieta Jastrzębska,[1] Urszula Bazylińska,[2] Magdalena Bułka,[1]
Katarzyna Tokarska,[1] Michał Chudy,[1] Artur Dybko,[1] Kazimiera Anna Wilk,[2]
and Zbigniew Brzózka[1,a)]
[1]*Institute of Biotechnology, Department of Microbioanalytics, Faculty of Chemistry,*
Warsaw University of Technology, Noakowskiego 3, 00-664 Warsaw, Poland
[2]*Department of Organic and Pharmaceutical Technology, Faculty of Chemistry,*
Wroclaw University of Technology, Wybrzeże Wyspiańskiego 27, 50-370 Wrocław, Poland

The application of nanotechnology is important to improve research and development of alternative anticancer therapies. In order to accelerate research related to cancer diagnosis and to improve the effectiveness of cancer treatment, various nanomaterials are being tested. The main objective of this work was basic research focused on examination of the mechanism and effectiveness of the introduction of nanoencapsulated photosensitizers to human carcinoma (A549) and normal cells (MRC-5). Newly encapsulated hydrophobic indocyanine-type photosensitizer (i.e., IR-780) was subjected to *in vitro* studies to determine its release characteristics on a molecular level. The photosensitizers were delivered to carcinoma and normal cells cultured under model conditions using multiwell plates and with the use of the specially designed hybrid (poly(dimethylsiloxane) (PDMS)/ glass) microfluidic system. The specific geometry of our microsystem allows for the examination of intercellular interactions between cells cultured in the microchambers connected with microchannels of precisely defined length. Our microsystem allows investigating various therapeutic procedures (e.g., photodynamic therapy) on monoculture, coculture, and mixed culture, simultaneously, which is very difficult to perform using standard multiwell plates. In addition, we tested the cellular internalization of nanoparticles (differing in size, surface properties) in carcinoma and normal lung cells. We proved that cellular uptake of nanocapsules loaded with cyanine IR-780 in carcinoma cells was more significant than in normal cells. We demonstrated non cytotoxic effect of newly synthesized nanocapsules built with polyelectrolytes (PEs) of opposite surface charges: polyanion—polysodium-4-styrenesulphonate and polycation—poly(diallyldimethyl-ammonium) chloride loaded with cyanine IR-780 on human lung carcinoma and normal cell lines. However, the differences observed in the photocytotoxic effect between two types of tested nanocapsules can result from the type of last PE layer and their different surface charge. © *2016 AIP Publishing LLC*. [http://dx.doi.org/10.1063/1.4941681]

INTRODUCTION

Lab-on-a-chips have now become accepted tools used for fundamental biological studies as they enable one to perform highly controlled *in vitro* experiments. A number of devices for the cell cultivation, single-cell, migration analysis, and cell based toxicity tests are reported.[1–3] In the microsystems, cells can be easily manipulated, and cellular environment can be precisely controlled.[4] Besides, there are also commercial microfluidic systems dedicated for cell

---

a)Author to whom correspondence should be addressed. Electronic mail: brzozka@ch.pw.edu.pl

engineering. The applications of the microfluidic systems are becoming wider and wider: starting with simple toxicity tests, through the use them for new drugs discovery, analysis, and matching of delivery methods, up to advanced diagnostics at the cellular level.[5,6] Probably in the future, we will take the advantage of them in the development of tissue engineering, including organ assist and organ replacement.[7–9] Important advantage of the microfluidic systems is the option of designing of their structures, according to the specific customer requirements. This allows targeting of cells, for example, in accordance with the designed geometry of the microchannels, and control or evaluate of various cell behaviors as cell-cell interactions, or biochemical signaling.[8,10]

The use of microfluidic systems for toxicity studies and cellular engineering is supported by a lot of examples. Huh *et al.* presented a microfluidic system that reconstitutes the functional surface of the human lung and checked a possibility of its application in nanotoxicological tests.[11] Kim *et al.* designed a microfluidic system for evaluation of silica nanoparticles' cytotoxicity towards human intestinal epithelial cells (Caco-2).[12,13] Also a microfluidic platform for anticancer drug testing was developed. Sung *et al.* studied drug effectiveness in a microchip on three different cell types: cultures of liver, tumor, and marrow cells at the same time.[14] The microsystems designed for the evaluation of the efficiency of other methods of the fight against cancer, e.g., photodynamic therapy (PDT), can also be applicable. The effectiveness of PDT is based on three independent factors: a photosensitizer (PS), intracellular oxygen, and light that is absorbed by the photosensitizer.[15] The examination of PDT procedure on the normal and carcinoma cells cultured in the separated and the "mixed" culture can also be performed using the microfluidic systems.[16]

The application of nanotechnology is important to improve research and development of alternative anticancer therapies. In order to accelerate research related to cancer diagnosis and to improve the effectiveness of cancer treatment, various nanomaterials are being developed.[17] Recently, the microsystems have become popular tools for nanoparticles' testing, e.g., to determine their stability, toxicity, or physico-chemical and biological properties. Mahto *et al.* presented a *lab-on-a-chip* system for the analysis of the toxicity of quantum dots. The authors checked the effect of Cd-Se/Zn-Se quantum dots on the BALB/3T3 cell line.[18]

Nanoparticles allow modification of the properties of photosensitizers used in photodynamic therapy. Scientists proved that various nanomaterials in combination with the photosensitizers may not only improve the efficiency of photodynamic therapy but also reduce the side effects.[17,19] Nanoparticles can increase the effectiveness of PDT, because they prevent from the aggregation of the photosensitizer, improve the mechanism of absorption of the chemical compound by the cells or completely eliminate this necessity by spontaneous singlet oxygen production.[20] Same nanoparticles may protect the photosensitizer against cellular environment, e.g., destructive enzymes. Thereby, significant improvement of the stability and other pharmacokinetic properties of the photosensitizers is observed.[21] On the other hand, some methods using nanoparticles, such as photosensitizer encapsulation, protect the non-cancer cells against the adverse effects of a photoactive drug.

The developed nanoparticles may have dimensions (50–150 nm) preventing their penetration into normal cells, which is difficult in case of soluble photosensitizers used as a solution.[21,22] The nanoparticles' dimension manipulation is one of the method, which extort, so-called, active targeting. Its purpose is selective penetration of photosensitizers' molecules to carcinoma cells.[22,23] Selectivity of the applied photosensitizers is increased by the surface modification of the nanoparticles.[19]

The photosensitizers may be combined with the nanoparticles in different ways, but encapsulation is one of the most effective methods. Earlier investigations related to encapsulation of a photosensitizing dye—methylene blue, have shown that loading the photosensitizers into microenvironments of polymeric nanocarriers may successfully protect the photoactive chemical compound from both any enzymatic degradation, and sudden changes in the environmental factors including temperature and/or pH.[24] This method also reduces the toxicity of the photoactive compound. This is of particular importance for healthy cells, when using this compound as a photosensitizer in anticancer therapy. Moreover, encapsulation allows binding of different

ligands to the surface of nanoparticles. This may intensify the active targeting process.[25] Some methods of encapsulation allow for controlled, continuous release of different compounds, for example, their encapsulation in biodegradable polymeric nanoparticles.[26] This allows checking the effect of continuous release of the photosensitizer on the effectiveness of PDT procedure.

The development of novel types of micro- and nanocontainers is constantly one of the main frontiers in the scientific research. In the last few years, the major progress has been achieved in the template-based approaches to produce a variety of hydrophobic drug-loaded nanocarriers for drug delivery, diagnostics, or other biomedical applications.[27,28] One of the most versatile methods of formation of nanostructured functional coatings on colloidal cores, including the oil one, comprises the sequential adsorption of polyelectrolytes (PEs) called the layer-by-layer (LbL) technique.[29–32] Among many micellar aggregates and their mediated polymeric systems, biocompatible long-sustained release oil-core polyelectrolyte nanocarriers are used. They are fabricated by the subsequent multilayer adsorption of PE at the micellar structures. Among them, oppositely charged polyelectrolytes have been found to successfully encapsulate indocyanine-type hydrophobic photosensitizers in order to target cells and avoid drug degradation and toxicity. It also allows improving drug's efficacy, its stability, and better intracellular penetration, owing to their enhanced permeation, specific cell targeting, and long circulation in blood stream.[31–35]

We have selected a NIR heptamethine indocyanine dye (i.e., IR-780 iodide) as a model hydrophobic photosensitizer basing mainly upon its excellent optical properties and good photosensitizing attributes. IR-780 indocyanine due to its characteristic *excitation* ($\lambda_{exc.} = 779$ nm) and emission ($\lambda_{em.} = 805$ nm) wavelengths and high molecular extinction coefficient ($\varepsilon = 27.4 \times 10^4 \, M^{-1} \, cm^{-1}$) has been adopted so far as a non-targeting contrast agent in clinical and experimental NIR imaging and as a promising second generation photosensitizer in PDT.[36–39] However, IR-780 as many other hydrophobic cyanines can be disposed to light-induced decomposition (i.e., photobleaching) both *in vitro* and *in vivo* resulting in the loss of absorbance, fluorescence, and photoactivity, and thus possibly limiting its use in PDT.[40] In order to increase the potential of hydrophobic cyanines towards improvement of drug efficacy, its stability, and better intracellular penetration, they need to be encapsulated in nanocarriers to avoid any unexpected problems with photoactivity and to improve their dissolution performance by means of encapsulation via template-mediated processes.[27,37]

The main objective of this work is a basic research focused on examination of the mechanism and effectiveness of the introduction of a photosensitizer to carcinoma cells in the form of nanocarriers such as PE nanocapsules and then performing cytotoxicity tests during photodynamic therapy based on the use of model conditions and designed system *lab-on-a-chip*. Newly encapsulated hydrophobic indocyanine-type photosensitizer (i.e., IR-780) was subjected to *in vitro* studies to determine its release characteristics on a molecular level. In addition, we tested the cellular internalization of nanoparticles (differing in size, surface properties) in carcinoma and normal lung cells.

MATERIAL AND METHODS

Most of the starting materials were purchased from Aldrich or Fluka and used as received. Other reagents and solvents were of commercial grade and were not additionally purified before the use. Cyanine-type photosensitizer: IR-780 iodide, human serum albumin (HSA), oleic acid (OA), as well as *polyelectrolytes of opposite charges:* polyanion—polysodium 4-styrenesulphonate (PSS, Mw 70 kDa) and polycation—poly(diallyldimethyl-ammonium) chloride (PDADMAC, Mw 100–200 kDa) were obtained from Sigma-Aldrich. Surfactant: *N,N*-bis[3,3′(trimethylammonio)-propyl]dodecanamide dimethylsulfate ($C_{12}(TAPAMS)_2$) was synthesized according to the method described in previously.[35] Water used for all experiments was distilled and purified by using of a Millipore (Bedford, MA) Milli-Q purification system.

Preparation of polyelectrolyte nanocapsules loaded with IR-780 cyanine

Both IR-780 cyanine-loaded and empty nanocapsules were prepared by a direct LbL saturation method described in our previous study.[34] Commonly, in the case of the loaded

TABLE I. Characteristics of IR-780-loaded and empty nanocapsules prepared by LbL approach.

No.	System name	D_H (nm)[a]	PdI[b]	ζ (mV)[c]	C_{IR-780} (μM)[d]	EE (%)[e]
1	C_{12}(TAPAMS)$_2$/OA/water(PDADMAC/PSS)$_{3.5}$(**nanocapsules 1**)	96	0.11	−42	empty	…
2	C_{12}(TAPAMS)$_2$/OA/water(PDADMAC/PSS)$_{3.5}$ (**nanocapsules 1**)	106	0.16	−41	78.1	97
3	C_{12}(TAPAMS)$_2$/OA/water(PDADMAC/PSS)$_4$(**nanocapsules 2**)	99	0.14	+56	empty	…
4	C_{12}(TAPAMS)$_2$/OA/water(PDADMAC/PSS)$_4$ (**nanocapsules 2**)	111	0.18	+59	60.1	95

[a]Hydrodynamic diameter (DH) determined by dynamic light scattering.
[b]Polydispersity index (PdI) determined by dynamic light scattering.
[c]Zeta potential (ζ) measured by the microelectrophoretic method.
[d]Concentration ($CIR-780$) of encapsulated cyanine.
[e]Encapsulation efficiency [EE].

nanocapsules, the hydrophobic photosensitizer IR-780 was, in the first step, dissolved in oleic acid (0.2 mg/ml) prior to emulsification with C_{12}(TAPAMS)$_2$. Next, the oil-core nanoemulsion templates were covered via the LbL adsorption of oppositely charged polyelectrolytes: anionic PSS and cationic PDADMAC to form multilayer shell nanocapsules. Solutions of the selected PE's (of concentration equal to 2 g/dm^3) were prepared by dissolving each polyion in NaCl solution of ionic strength 0.015 M without any pH adjustment. The optimal ratio of empty and loaded nanoemulsion to polyion concentrations was determined by measuring zeta potential of formed nanocapsules and investigating their stability.

Characterization of nanocapsule size, surface charge, and morphology

The zeta potential (ζ-potential) of nanoemulsion templates and nanocapsules was measured by the microelectrophoretic method using a Malvern Zetasizer Nano ZS apparatus according to the method described previously.[41] Each value of ζ-potential was obtained as an average of three subsequent runs of the instrument with at least 20 measurements. The size distribution (i.e., the hydrodynamic diameter) of the nanosystems was determined by Dynamic Light Scattering (DLS) using Zetasizer Nano Series from Malvern Instruments with the detection angle of 173° in optically homogeneous square polystyrene cells. All measurements were performed at 25 °C. Each value of hydrodynamic diameter was obtained as an average of three runs with at least 10 measurements. The DTS (Nano) program was applied for data evaluation. The corresponding hydrodynamic diameter (D_H) and polydispersity index (PdI) are listed in Table I with the ζ-potential values. The imaging of the obtained nanocapsules was investigated by scanning electron microscopy (SEM) and atomic force microscopy (AFM) according to detailed procedure described our earlier studies.[33] In the case of SEM observation, the shape and morphology of the dry nanocapsules were investigated by field emission SEM (JEOL JSM-7500 F), at an operation voltage of 15 keV. The samples were prepared by placing a drop of nanocapsules suspension on the copper cylinders and drying overnight. The morphology of the nanocapsules was checked using the Veeco NanoScope Dimension V AFM with an RT ESP Veeco tube scanner. The scanning speed was 0.5 Hz, and a low-resonance-frequency pyramidal silicon cantilever resonating at 250–331 kHz was employed (at a constant force of 20–80 N/m). The nanocapsules were allowed to adsorb on a freshly cleared mica surface for 24 h by dipping it in the suspension and then removing the excess of substrate by rinsing mica plates with double distilled water and drying at room temperature.

Encapsulation and photobleaching of IR-780 cyanine

Encapsulation efficiency (EE) of multilayer nanocapsules and photobleaching study of the free and encapsulated IR-780 was determined spectrophotometrically using UV-Vis Spectrophotometer U-2900 (Hitachi) according to the detailed protocols described in our previous studies.[39] All the irradiation experiments were performed using an OPTEL Fibre Illuminator (Opole, Poland) equipped with a band pass glass filter (SCHOTT GLASWERKE

GmbH) to isolate the 760–800 nm spectral interval. The rate of photobleaching was evaluated by measuring the cyanine absorption spectrum in the 500–800 nm range upon exposure of 3 ml solutions containing 4 μM IR-780 or its encapsulated form to the lamp operating at the energy dose of 100 mW/cm^2. The solutions were irradiated in open 1 cm quartz cuvettes with continuous stirring. The absorbance measurements were carried out every 2 min during the irradiation.

Cellular uptake

Human lung carcinoma (A549) and human fetal lung fibroblast (MRC-5) cells were obtained from American Type Culture Collection and European Type Culture Collection. The cells were cultured in Dulbecco's Modified Eagle's Medium (DMEM) medium (Sigma Aldrich) supplemented with 10%$_{v/v}$ fetal bovine serum (Gibco), 1%$_{v/v}$ streptomycin and penicillin (Sigma Aldrich) in a humidified atmosphere (5% CO_2, 37 $^\circ$C).

The flow cytometry analysis (FACS) was performed for quantitative testing of intracellular uptake of IR-780 cyanine by A549 and MRC5 cells. For this purpose, 70% confluent cell cultures were incubated for 24 h with 4 μM of free (native) and encapsulated IR-780 cyanine. The cells incubated with culture medium and comparative amounts of nanocapsules without cyanine were used as control samples. Next, the cells were detached and washed twice with phosphate buffer solution (PBS). Finally, the cells suspended with 1 ml PBS were analyzed using FACS (Becton Dickinson) equipment with an argon laser (488 nm) and red-diode laser (635 nm). After excitation of samples at 635 nm, the fluorescence emission intensity was measured using a 661/16 nm band pass filter. The data were analyzed using CellQuest software and presented as single-parameter histograms and geometric mean (GMean) of fluorescence intensity.

Cellular internalization

The A549 and MRC-5 cells were seeded on cell culture dishes with glass bottom (CELL view^{TM}, Greiner bio-one) and incubated with nanocapsules for 24 h. Next, the cells were examined under the confocal scanning laser microscope (FLUOVIEW FV10i-LIV Confocal Laser Scanning Microscope, Olympus) by using a 635 nm excitation filter. The data were analyzed using Fluoview FV10i software (Olympus).

Microsystem geometry

Cytotoxicity and photocytotoxicity (evaluation of PDT procedures) were analyzed in a microfluidic platform (Fig. 1). The microsystem was made of PDMS (Sylgard 184, Dow
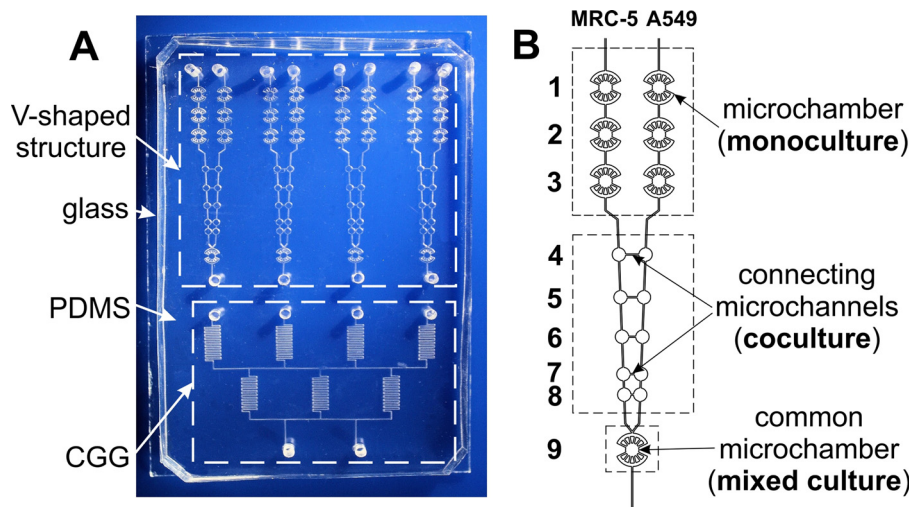

FIG. 1. Photo of the microsystem (a), scheme of the microchambers connected with the microchannels (b).

Corning) and a sodium glass plate (Helmand, 75 mm $\times$ 55 mm $\times$ 0.5 mm). Microstructures in PDMS were fabricated using a photolithography and replica molding techniques according to the protocols described in our previous work.[42] To obtain the sealed microsystem, PDMS and glass plates were bonded using surface plasma activation (Plasma Preen System Inc. II 973).

The geometry of used microsystem was based on the design presented in our previous work.[16] The microsystem consists of four microstructures with a network of microchannels which are arranged in V-shaped configuration. Each V-shaped microstructure provided various types of cell cultures: monoculture, coculture, and mixed culture (see Fig. 1(b)). Monocultures of two different cell lines were performed in three pairs of the microchambers, without any additional (connecting) microchannels. The next five microchambers (connected with microchannels having a length of: 1000, 800, 600, 400, and 200 μm, respectively) provided cocultures of cells and cells' migration analysis along the connecting microchannels. The mixed culture was obtained in the common microchamber, in which two cell lines were seeded side by side, simultaneously. The geometry of the microsystem also consists of a concentration gradient generator (CGG). Thanks to this, in V-shaped structures four different concentrations of tested photosensitizer in a single step can be evaluated.

Cytotoxicity assays

Macroscale

Two kinds of nanocapsules, dependent on the number of polyelectrolyte layers: $C_{12}(TAPAMS)_2/OA/water(PDADMAC/PSS)_{3.5}$ (we called as **nanocapsules 1**) and $C_{12}(TAPAMS)_2/OA/water(PDADMAC/PSS)_4$ (we called as **nanocapsules 2**), were investigated (Table I). Empty (unloaded) and loaded with cyanine IR-780 **nanocapsules 1** and **nanocapsules 2** were prepared in DMEM culture medium at concentration range of 0–6 μM. Moreover, 400 μM stock solution of free IR-780 cyanine (native sample) was prepared in ethanol. Next, the final concentration (0–6 μM) of free cyanine was obtained by dilution in DMEM. Culture medium without cyanine and solution of **empty nanocapsules 1** and **empty nanocapsules 2** were used as control samples.

A549 and MRC5 cells were seeded at a density of 10^4 cells/well in DMEM on 96-well plates and incubated for 24 h in the CO_2 cell culture incubator. After that time, the medium in the wells was replaced with 200 μl of the tested samples (empty and loaded **nanocapsules 1, 2** with cyanine IR-780 as well as free IR-780 cyanine solution), prepared according the procedure described above. Next, the cells were incubated overnight. Finally, the cytotoxicity of empty and loaded nanocapsules as well as a free cyanine was investigated using MTT assays (Invitrogen) according to the protocol suggested by the manufacturer.

The microsystem

Before the cell culture, the microsystem was prepared according to the protocol described in our previous work.[16] Next, 2×10^6 cells ml^{-1} A549 and MRC5 cell suspensions were seeded through two V-shaped inlets of each V-shaped microstructure (a flow rate of 5 μl min^{-1}) using the peristaltic pumps (Ismatec Reglo-Digital MS-4/12) (Fig. 1). The microsystems with A549 and MRC5 cells, cultured for 24 h in V-shaped structures (Fig. 1(b)), were utilized for cytotoxicity and photocytotoxicity tests. The tested solutions (6 μM of cyanine-loaded **nanocapsules 1, 2**, or free cyanine) and DMEM medium (as a control solution) were introduced through two CGG inlets with a flow rate of 5 μl min^{-1} for 10 min. After passing the CGG microchannels, four different concentrations of the tested photosensitizers (0, 2, 4, and 6 μM) were obtained. Next, the microsystem was sealed and placed for 24 h in the CO_2 incubator.

After that time, cytotoxicity tests or PDT procedures (light irradiation) were performed. For PDT procedures, the cells were irradiated through the PDMS layer using a high power light-emitting diode (LED) (a distance of 10 mm, time 10 min, $\lambda = 780$ nm, energy dose 6.5 mW/cm^2 and 10 mW/cm^2). The viability of the cells was determined 24 h after the incubation with the photosensitizer or after the PDT procedures. Cyto- and photocytotoxicity were

investigated using calcein AM (CAM, Sigma Aldrich) and propidium iodide (PI, Sigma Aldrich) for cells' staining. The "*cellSens Dimension*" image analysis software (Olympus) was used for data acquisition and analysis. Experimental data are expressed as mean ± standard deviation (SD) from at least four independent experiments.

RESULTS AND DISCUSSION

Fabrication and characterization of IR-780 loaded polyelectrolyte multilayer nanocapsules

In any nanocarrier preparation method, special attention has to be paid on the aspects determining the container features responsible for the best attainment of the final goal. Improving cellular uptake, solubility and release of active molecules, stability of the colloidal system and its protection from the aggregation in aqueous media, can be realized by the use of charged multilayer container shells.[29] Therefore, the oil-core PE shell nanocapsules obtained by the LbL approach can be considered as suitable containers for a variety of insoluble in water, hydrophobic cargoes. Being composed of the liquid core (e.g., nanoemulsion or emulsion oil droplets), which is surrounded by the multilayer polyelectrolyte shell forming a sort of a shield that protects the loaded core from the surrounding medium, in particular, from decomposition of the given ingredient during long storage or delivery to the targeted site. Moreover, it is possible to fabricate the designed cargo-loaded multilayer nanocapsules with a good control of size (e.g., to get the nanoproducts ca. 150 nm in diameter) and desirable shell properties. The latter corresponds to the nanocapsules with hydrophilic surfaces, including functionalized, that is capable of appreciable surface interactions with biological systems (treated as high biocompatibility) and improved accumulation in tumor tissues.[43,44] Additionally, due to the presence of multilayer shield, encapsulated therapeutic molecules can be protected from the biological environment. Moreover, their bioavailability and biodistribution can be enhanced. Consequently, the formation of the multilayer polyelectrolyte nanocapsule shells was performed by subsequent adsorption of PSS/PDADMAC polyelectrolytes from their solutions without the intermediate rinsing step, according to the LbL procedure for the nanoemulsion-templated approach described in detail in Material and Methods section. It was established that surface charge and composition of nanocapsules are among the most important physical and chemical factors influencing the toxicological effects and success of polyelectrolyte nanocapsules interactions with cells.[29] Therefore, for our study, we have chosen the multilayer nanocapsules with different PE shell type (terminated by PDADMAC or PSS) and loaded by various concentration of IR-780 cyanine dye. The composition and physicochemical properties of both empty and cyanine-loaded nanoemulsion-templated nanocapsules are summarized in Table I. The surface charge was determined by ζ-potential measurements and as it has been proved in our previous studies, the stable nanostructures were obtained when the zeta potential of nanocarriers with the adsorbed PE layer was close to the zeta potential of the same polycation or polyanion in solution.[34,35] Consequently, the volumes of polyelectrolyte solution used to form each layer of nanocapsules shell were determined experimentally by the evaluation of the results of simultaneous zeta potential measurements. The results of ζ-potential measurements during the LbL deposition are typical zigzag dependence used as evidence for the formation of consecutive layers and stability of the obtained nanocapsules. The values of the ζ-potential oscillated from -42 to $+58$ mV for PDADMAC/PSS polyelectrolyte pairs. It proved that the obtained capsules shells were stable with zeta potential ranges for PSS and PDADMAC layers.

As it has been reported previously,[29] the most suitable size and narrow size distribution of a drug delivery system are the key factor in their biodistribution and prolonged circulation followed by the accumulation in the tumor tissues. The effective drug delivery system should have a diameter between 100 and 200 nm to avoid clearance by first pass renal filtration as well as detection by the phagocytic system and consequently achieve a longer circulation time in the bloodstream.[28] In our study, the average size (hydrodynamic diameters, D_H) of the obtained multilayer nanocapsules was dependent on the number of PE layers (Table I) and ranged from 96 nm (**empty nanocapsules 1**) to 111 nm (**loaded nanocapsules 2**). The example of the DLS

size distribution graph for IR-780-loaded **nanocapsules 1** is presented in Fig. 2(a). The suspensions were reasonably monodisperse (low values of PdI < 0.25), which made them good candidates for anticancer therapies. Imaging of the obtained nanocapsules by SEM and AFM technique proved its roughly spherical and moderately uniform shape (Figs. 2(b) and 2(c)). Furthermore, the nanocarriers do not show any enhanced aggregation, and non-loaded crystals of IR-780 cyanine present on the nanoparticles outer surface were not detected. The average size of the most observed particles is around 100 nm, which is in good agreement with the values obtained by DLS in the wet conditions (Fig. 2(a)).

Moreover, UV-Vis spectroscopy was used to demonstrate both the encapsulation of IR-780 cyanine into liquid cores covered by polyelectrolyte shells as well as to estimate its photobleaching rate in comparison to the native (non-loaded) dye form (see Fig. S1).[45] Along with spectrophotometric analysis, we detected that IR-780 is loaded into the nanocapsules liquid core with high drug EE between 90% and 97% (Table I).

Fig. S1(a) demonstrates the UV–Vis spectra of IR-780-loaded **nanocapsules 1** compared with the spectrum for empty ones and the spectrum of the photosensitizer dissolved in acetone-water mixture (acetone: $H_2O = 1:1$).[45] The characteristic peak at 786 nm has been observed in the case of freshly prepared cyanine-loaded nanocarriers (higher absorbance was noted in acetone: H_2O sample containing the same concentration of IR-780). This proves that the photosensitizer was enclosed inside of nanocarriers. Furthermore, the spectrum of dye-loaded nanocarriers is not significantly changed after three months storage of the nanocapsules in the dark. It gives the evidence for long-term photostability and the enclosure of cyanine-dye into liquid cores covered by polyelectrolyte shells. As it has been mentioned, the use of indocyanines as effective photosensitizers may be limited by their photobleaching, resulting in the loss of their photoactivity.[40] Our experiments, performed under conditions similar to that described before, prove that encapsulation of the IR-780 in the oil-core multilayer nanocapsules reduces the photobleaching and thus enhances its photodynamic effectiveness. Fig. S1(c) shows the absorbance
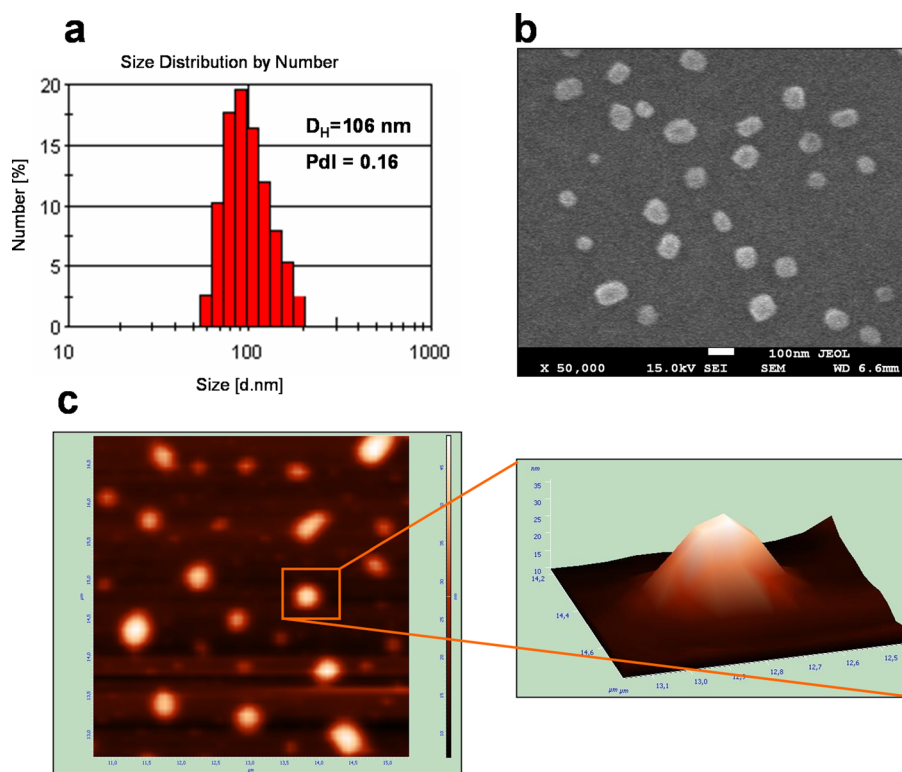

FIG. 2. Characteristics of IR-780-loaded **nanocapsules 1** along with DLS (a), SEM (b), and AFM (c). Example for $C_{12}(TAPAMS)_2$/OA/water(PSS/PDADMAC)$_{3.5}$ (see the row 2 in Table I).

changes of the cyanine encapsulated in the all studied types of nanocapsules compared to solution containing free IR-780 as a function of irradiation time.[45] In agreement with *the three-phase process behavior*,[46] the cyanine molecules loaded in multilayer nanocarriers exhibited better photostability during irradiation than the respective free dye. Furthermore, IR-780 encapsulated by nanoemulsions covered by four PE bilayers (**nanocapsules 2**) photobleaches slightly lower than when enclosed in nanocapsules with thinner coat (**nanocapsules 1**) (see Table I). The observed phenomenon confirmed the earlier *findings,*[33,39] *indicating that both the nanoparticles' oil core and PE shell thickness may significantly enhance the photostability of the hydrophobic photosensitizer. Other important in vitro* features of the encapsulated IR-780 such as reactive oxygen species (ROS) and release characteristics are supplemented in the supplementary material (Figs. S2 and S3).[45]

Cellular uptake

Flow cytometry allows determining the qualitative and quantitative accumulation of PS encapsulated in nanocarriers, based on the fluorescence emitted by the PS after excitation with a specific wavelength of light. This technique has been used in the similar study of cellular internalization, which showed the concentration and time dependences of cyanine PS' accumulation.[47]

The results presented in Fig. 3 show the cellular uptake of free cyanine IR-780 and **nanocapsules 1** and **2**. The analysis carried out using flow cytometry demonstrated accumulation of the photosensitizers in A549 and MRC-5 cells. We observed a significant increase in the fluorescence signal emitted from cells treated with the nanocapsules 1 and 2 in relation to the residual autofluorescence of untreated cells (G_{mean} from 3 to 8 a.u. for A549 and MRC-5 cells, respectively). As control samples, we used A549 and MRC-5 cells untreated with cyanine IR-780.

Moreover, the accumulation of IR-780-loaded **nanocapsules 1** and **2** in carcinoma cells was about 4 times higher than in normal cells. It indicates that the synthesized nanocapsules can be successfully used as potential delivery systems of hydrophobic photosensitizers to the carcinoma target cells. For nanocapsules 2, slightly higher fluorescence signal was observed. It can be assigned to the type of last PE layer in synthesized nanocapsules. This may be the total effect of both nanocarriers structure and the surface charge of the nanocapsules as similarly observed in our previous FACS study for MCF-7/WT cells treated by IR-786-loaded nanocapsules with different $(PSS/PDADMAC)_n$ shell.[33]

On the other hand, the cellular uptake of free cyanine IR-780 in A549 cells was almost 2 times higher in relation to the **nanocapsules 1** and **2**. While in the case of MRC-5 cells we observed an inverse trend, cellular uptake of free cyanine IR-780 was almost 2 times lower.

Cellular internalization

The confocal microscope imaging was performed to evaluate if there would be an increased intracellular distribution of photosensitizers' nanocapsules in A549 and MRC-5 cells.
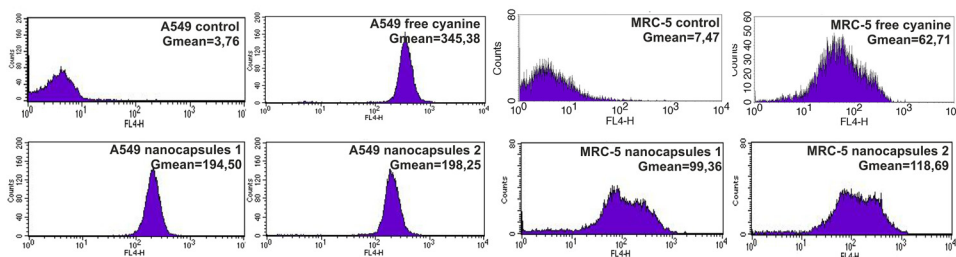

FIG. 3. Distributions of fluorescence intensity of A549 and MRC-5 cells incubated with three different forms of cyanine IR-780. The cells were exposed to 4 μM of free cyanine and 4 μM of **nanocapsules 1** and **2** for 24 h. On the graph, the geometrical means (G_{mean}) of red fluorescence intensity are displayed in the inset.

After 24 h of incubation with **nanocapsules 1** and **2**, we observed multiple fluorescent points at the carcinoma and normal cells' membrane surfaces (Fig. S4).[45] This indicates that the both **nanocapsules 1** and **2** efficiently localize throughout the cytoplasm in A549 and MRC-5 cells. As control samples we used untreated cells of both lines.

Cytotoxicity tests in a macroscale

One of the most important criteria that must be fulfilled by the photosensitizer is that it must not cause acute cytotoxicity. For this purpose, the safe range of photosensitizers' concentrations to the cells was determined. Therefore, MTT assay was used for the quantitative viability determination of the A549 and MRC-5 cells treated with different forms of cyanine IR-780.

Based on the MTT viability assays, we explored that free cyanine IR-780 and **nanocapsules 1** and **nanocapsules 2** (tested concentrations: 2, 4, and 6 μM) did not show cytotoxic effect on both A549 and MRC-5 cell lines after 24 h of incubation (Fig. 4). The carcinoma and normal cells viability was approximately 90%–100% for all the tested forms of the photosensitizer.

Cytotoxicity and photocytotoxicity tests in the microsystem

After the investigation of cellular uptake, internalization and optimization of non cytotoxic range of cyanine IR-780 concentrations in the macroscale, we performed cyto- and photocytotoxicity tests of free cyanine and nanocapsules 1 and 2 in the microsystem.
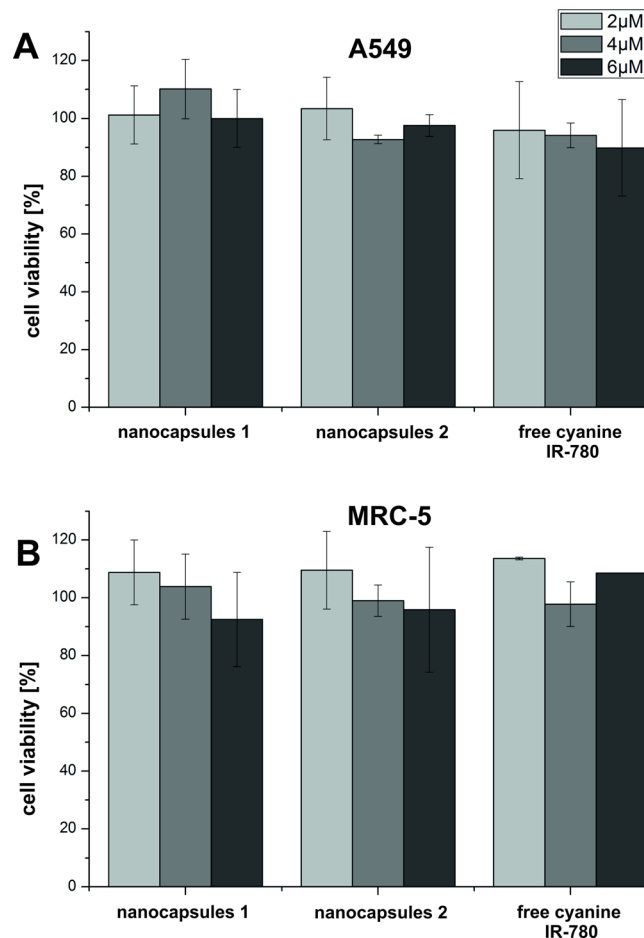

FIG. 4. (a) A549 and (b) MRC-5 cells viability after 24 h incubation with **nanocapsules 1** and **nanocapsules 2** and free cyanine IR-780.
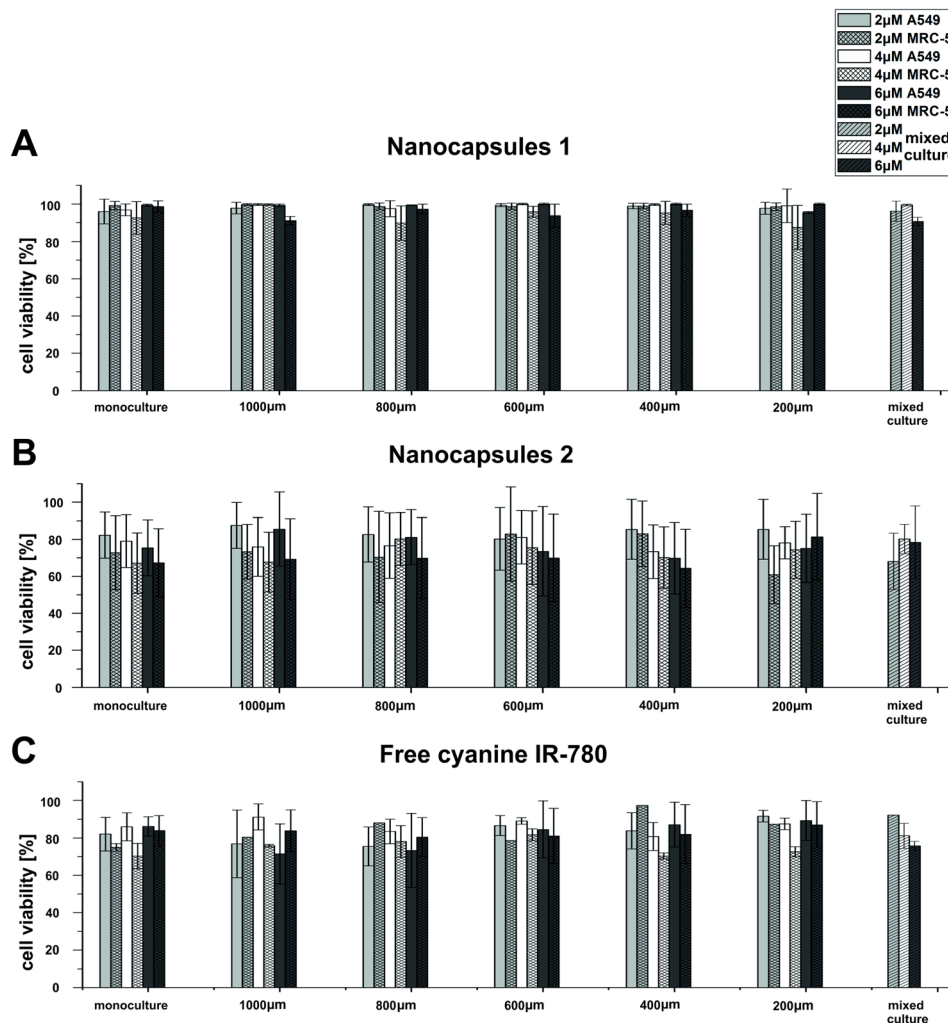
FIG. 5. A549 and MRC-5 cells viability after 24 h of incubation with **nanocapsules 1** (a) and **nanocapsules 2** (b) and free cyanine IR-780 (c) and after 24 h of carried out PDT procedures ($\lambda = 780$ nm, energy dose 6.5 mW/cm^2, t $= 10$ min) for monoculture, coculture, and mixed culture.

The use of the chip (Fig. 1) enabled one step analysis of different types of culture: monoculture, coculture, and mixed culture of carcinoma A549 and normal MRC-5 cells. This allowed conducting additional studies of cytotoxicity and photocytotoxicity not only on separate cell lines but also on coculture (such tests were not possible in the macroscale). This was based on the normal and carcinoma cells culture in microchambers with precisely defined distances (connecting microchannels) between them (Fig. 1(b)).

The results of cyto- and photocytotoxicity tests of the **nanocapsules 1** and **2** and free cyanine IR-780 are presented separately in Figs. 5(a)–5(c), respectively. The cells' viability was calculated for each microchamber after 24 h of cyanine IR-780 treatment (cytotoxicity tests) and 24 h after the irradiation (photocytotoxicity tests). Moreover, exemplary photographs of A549 and MRC-5 cells stained with CAM and PI for viability evaluation after PDT procedure are shown in the supplementary material.[45] In addition, cell viability for A549 and MRC-5 cells in the mixed culture (common microchamber, Fig. 1(b)) is presented without distinguishing the cell lines. Similar to the macroscale, research on the free cyanine and **nanocapsules 1** and **nanocapsules 2** (tested concentrations: 2, 4, and 6 μM) performed in the microsystem did not reveal cytotoxicity of photosensitizers to A549 and MRC-5 cells (data not shown). It proved that the designed microsystem can be applied for cytotoxicity tests, successfully. The main advantage of the proposed microfluidic-based platform is a possibility for creation of culture

conditions similar to *in vivo*. Thanks to the flow conditions as well as carcinoma-normal cell coculture (in precisely defined distances), it could be possible a deeper investigation how the presence of carcinoma cells influences normal cells after PDT procedures. Therefore, the photocytotoxicity of the tested photosensitizers were analyzed in the microsystem (Fig. S5).[45]

Following the PDT procedures (irradiation at $\lambda = 780$ nm, energy dose 6.5 mW/cm^2, t = 10 min), there was no decrease in the viability of A549 and MRC-5 cells incubated with **nanocapsules 1** for each type of cell culture performed in our microsystem (Fig. 5(a)), while we observed a decrease in the viability (to the level of 75%–80% for A549 cells and 60%–65%
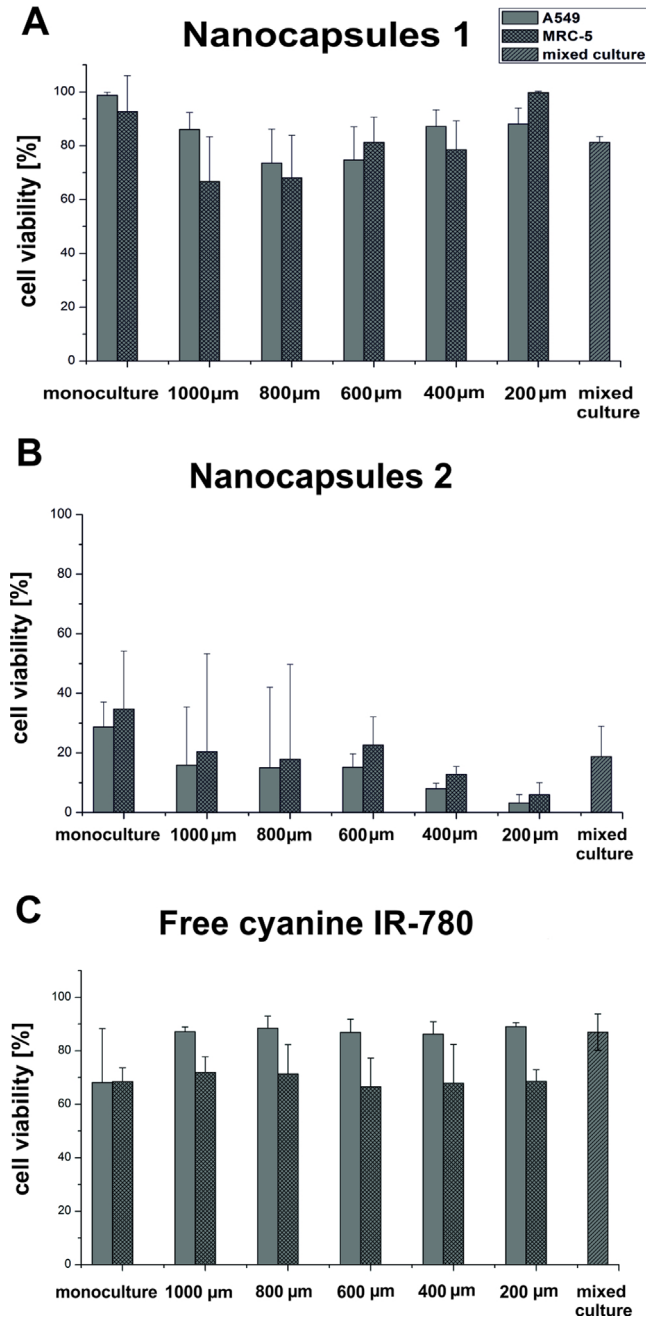

FIG. 6. A549 and MRC-5 cells viability after a 24 h incubation with the 6 μM of **nanocapsules 1** (a) and **nanocapsules 2** (b) and after 24 h of carried out PDT procedures ($\lambda = 780$ nm, energy dose 10 mW/cm^2, t = 10 min) for the monoculture, coculture, and mixed culture.

for MRC-5 cells) for monocultures of both carcinoma and normal cell lines incubated with **nanocapsules 2** (Fig. 5(b)). A IC50 (half maximal inhibitory concentration) for monoculture was determined. The IC50 value was high: $21 \mu M$ and $18 \mu M$ for A549 and MRC5 cells, respectively. The IC50 was determined by linear regression method using Microsoft Excel.

Cell viability analysis in coculture was performed for the next five rows of microchambers (Fig. 1(b)) connected together by the microchannels of precisely defined lengths (1000, 800, 600, 400, and 200 μm) allowed to assess the influence of culture medium diffusion between the microchambers on the normal and carcinoma cells' proliferation. Coculture tests are very difficult or almost not possible to perform by using conventional macroscale multiwell plates. For the coculture, as in the case of monocultures in the microsystem, the **nanocapsules 1** did not exhibit significant photocytotoxicity to carcinoma and normal cells after 24 h of incubation and 24 h after performing PDT procedures. Whereas we observed a decrease in A549 and MRC-5 cells viability (approximately to the level of 85% for carcinoma cells and 70% for normal cells) for the **nanocapsules 2**. Moreover, we observed similar photocytotoxic effect of **nanocapsules 2** in the mixed culture, as for the mono- and coculture. Whereas both carcinoma and normal cell lines incubated with free cyanine IR-780 showed relatively high viability after the PDT procedures (Fig. 5(c)). This indicates higher photocytotoxic effect of **nanocapsules 2** in comparison with free photosensitizer.

In the next stage of our research, the energy dose of irradiation was increased to 10 mW/cm^2, as we believed that this would enhance the photocytotoxicity effect of the tested nanocapsules. On the other hand, we decided to incubate cells with the tested photosensitizers at their concentration of 6 μM. It was the highest tested concentration of each type of the photosensitizer that only in case of **nanocapsules 1** did not exhibit any cyto- and photocytotoxic effect. The results of cell viability are shown in Fig. 6.

This time a slight decrease in the viability of both A549 and MRC-5 cell lines incubated with **nanocapsules 1** (Fig. 6(a)) was observed (the effect was higher than obtained previously for energy dose 6.5 mW/cm^2). However, a significant decrease in the viability of the tested cell lines treated with **nanocapsules 2** (Fig. 6(b)) was noted. For monoculture A549 and MRC-5 cells' viability was approximately 30% and 35%, respectively. On the other hand, for the connected microchambers cells' viability was a little bit higher for normal cells but for both cell lines it was less than 20%. There was a slight decrease trend of the both cell lines viability with diminishing distance between the microchambers. The lowest cells' viability was observed in the microchambers connected with the shortest microchannel. Based on these studies, it could be concluded that the increase of energy dose to 10 mW/cm^2 causes a significant decrease in the cell viability for **nanocapsules 2**, whereas for the **nanocapsules 1** photocytotoxic effect was not so high. We assume that these phenomena can result from the nanocapsules' surface charge difference so more detailed research will be conducted in the nearest future.

CONCLUSIONS

In this paper, we have investigated efficacy of nanoencapsulated indocyanine-type photosensitizers' delivery to the cell cultured under model conditions using multiwell plates and the specially designed hybrid (PDMS/glass) microfluidic system. The specific geometry of our microsystem allows for the examination of intercellular interactions between normal (MRC-5) and carcinoma cells (A549), cultured in the microchambers connected with microchannels of precisely defined length (200–1000 μm). Such a construction allows investigating various therapeutic procedures (e.g., PDT) on cells under similar to *in vivo* conditions. During our studies, the presented microfluidic system was used for determination of nanocarriers influence on three types of cell cultures: monoculture, coculture, and mixed culture, simultaneously, which is very difficult and time consuming to perform using standard 96-multiwell plates.

In our study, we demonstrated non cytotoxic effect of new synthesized nanocapsules built with polyelectrolytes of opposite surface charges: polyanion—PSS and polycation—PDADMAC loaded with cyanine IR-780 on human lung cell lines A549 and MRC-5. The long-term stability of new synthesized dye-loaded nanocarriers was proved by their UV-Vis spectra acquisition after

over three months storage. Moreover, flow cytometry and confocal microscope imaging were used to evaluate selective accumulation of nanocapsules in both cell lines tested. Our data showed that cellular uptake of nanocapsules loaded with cyanine IR-780 in carcinoma cells (A549) was more significant than in normal cells (MRC-5).

After advanced characterization of two types of nanocarriers (**nanocapsules 1** and **nanocapsules 2**), their photocytotoxicity was evaluated on two cell lines in the microfluidic system. The results obtained in microscale also proved low cytotoxicity of both tested nanosystems. In turn, decrease in the viability of both cell lines was noticed after PDT procedure for **nanocapsules 2**. The photocytotoxic effect observed for **nanocapsules 1** was not statistically significant. However, after increasing of applied energy during PDT procedure, the photocytotoxic effect observed was noticeable for **nanocapsules 1** and much higher for **nanocapsules 2** (cells' viability less than 20%). We suppose that the differences observed in the photocytotoxic effect between two types of tested nanocapsules can result from the last PE layer and its different surface charge. However, further studies are needed to explain this phenomenon and to improve the photocytotoxic effect of PE nanoencapsulated photosensitizer.

ACKNOWLEDGMENTS

[1]M. Ghanbari, A. S. Nezhad, C. G. Agudelo, M. Packirisamy, and A. Geitmann, J. Biosci. Bioeng. **117**, 504 (2014).
[2]P. Ertl, D. Sticker, V. Charwat, C. Kasper, and G. Lepperdinger, Trends Biotechnol. **32**, 245 (2014).
[3]E. Primiceri, M. S. Chiriacò, E. D'Amone, E. Urso, R. E. Ionescu, A. Rizzello, M. Maffia, R. Cingolani, R. Rinaldi, and G. Maruccio, Biosens. Bioelectron. **25**, 2711 (2010).
[4]J. Nilsson, M. Evander, B. Hammarström, and T. Laurell, Anal. Chim. Acta **649**, 141 (2009).
[5]D. B. Weibel and G. M. Whitesides, Curr. Opin. Chem. Biol. **10**, 584 (2006).
[6]N. T. Nguyen, S. A. Shaegh, N. Kashaninejad, and D. T. Phan, Adv. Drug. Delivery Rev. **65**, 1403 (2013).
[7]N. K. Inamdar and J. T. Borenstein, Curr. Opin. Biotechnol. **22**, 681 (2011).
[8]M. Hamon and J. W. Hong, Mol. Cells **36**, 485 (2013).
[9]C. Luni, E. Serena, and N. Elvassore, Curr. Opin. Biotechnol. **25**, 45 (2014).
[10]D. Kim, X. Wu, A. T. Young, and C. L. Haynes, Acc. Chem. Res. **47**, 1165 (2014).
[11]D. Huh, B. D. Matthews, A. Mammoto, M. Montoya-Zavala, H. Y. Hsin, and D. E. Ingber, Science **328**, 1662 (2010).
[12]P. M. Valencia, O. C. Farokhzad, R. Karnik, and R. Langer, Nat. Nanotechnol. **7**, 623 (2012).
[13]H. J. Kim, D. Huh, G. Hamilton, and D. E. Ingber, Lab Chip **12**, 2165 (2012).
[14]J. H. Sung, C. Kam, and M. L. Shuler, Lab Chip **10**, 446 (2010).
[15]P. Agostinis, K. Berg, K. A. Cengel, T. H. Foster, A. W. Girotti, S. O. Gollnick, S. M. Hahn, M. R. Hamblin, A. Juzeniene, D. Kessel, M. Korbelik, J. Moan, P. Mroz, D. Nowis, J. Piette, B. C. Wilson, and J. Golab, CA Cancer J. Clin. **61**, 250 (2011).
[16]E. Jastrzębska (Jędrych), I. Grabowska-Jadach, M. Chudy, A. Dybko, and Z. Brzózka, Biomicrofluidics **6**, 44116 (2012).
[17]G. V. Roblero-Bartolón and E. Ramón-Gallegos, Gac. Med. Mex. **151**, 78 (2015).
[18]S. K. Mahto, T. H. Yoon, and S. W. Rhee, Biomicrofluidics **4**, 034111 (2010).
[19]D. Bechet, P. Couleaud, C. Frochot, M. Viriot, F. Guillemin, and M. Barberi-Heyob, Trends Biotechnol. **26**, 612 (2008).
[20]F. Yan and R. Kopelman, Photochem. Photobiol. **78**, 587 (2003).
[21]R. Allison, H. Mota, V. Bagnato, and C. Sibata, Photodiagn. Photodyn. Ther. **5**, 19 (2008).
[22]F. Marcucci and F. Lefoulon, Drug Discovery Today **9**, 219 (2004).
[23]K. Cho, X. Wang, S. Nie, Z. G. Chen, and D. M. Shin, Clin. Cancer Res. **14**, 1310 (2008).
[24]W. Tang, H. Xu, E. J. Park, M. A. Philbert, and R. Kopelman, Biochem. Biophys. Res. Commun. **369**, 579 (2008).
[25]E. Paszko, C. Ehrhardt, M. O. Senge, D. P. Kelleher, and J. V. Reynolds, Photodiagn. Photodyn. Ther. **8**, 14 (2011).
[26]A. Kumari, S. K. Yadav, and S. C. Yadav, Colloids Surf., B **75**, 1 (2010).
[27]J. Nicolas, S. Mura, D. Brambilla, N. Mackiewicz, and P. Couvreur, Chem. Soc. Rev. **42**, 1147 (2013).
[28]B. Daglar, E. Ozgur, M. E. Corman, L. Uzun, and G. B. Dermiel, RSC Adv. **4**, 48639 (2014).
[29]K. Szczepanowicz, U. Bazylińska, J. Pietkiewicz, L. Szyk-Warszyńska, K. A. Wilk, and P. Warszyński, Adv. Colloid Interface Sci. **222**, 678 (2015).
[30]B. V. Parakhonskiy, A. M. Yashchenok, M. Konrad, and A. G. Skirtach, Adv. Colloid Interface Sci. **207**, 253 (2014).
[31]E. M. Shchukina and D. G. Shchukin, Curr. Opin. Colloid Interface Sci. **17**, 281 (2012).
[32]D. O. Grigoriev and R. Miller, Curr. Opin. Colloid Interface Sci. **14**, 48 (2009).
[33]U. Bazylińska, J. Pietkiewicz, J. Saczko, M. Nattich-Rak, J. Rossowska, A. Garbiec, and K. A. Wilk, Eur. J. Pharm. Sci. **47**, 406 (2012).
[34]U. Bazylińska, R. Skrzela, K. Szczepanowicz, P. Warszyński, and K. A. Wilk, Soft Matter **7**, 6113 (2011).
[35]U. Bazylińska, R. Skrzela, M. Piotrowski, K. Szczepanowicz, P. Warszyński, and K. A. Wilk, Bioelectrochemistry **87**, 147 (2012).
[36]G. Chapman, M. Henary, and G. Patonay, Anal. Chem. Insights **6**, 29 (2011).
[37]C. Zhang, T. Liu, Y. Su, S. Luo, Y. Zhu, X. Tan, S. Fan, L. Zhang, Y. Zhou, T. Cheng, and C. Shi, Biomaterials **31**, 6612 (2010).

[38]N. S. James, Y. Chen, P. Joshi, T. Y. Ohulchanskyy, M. Ethirajan, M. Henary, L. Strekowski, and R. K. Pandy, Theranostics **3**, 692 (2013).

[39]U. Bazylińska, A. Lewińska, L. Lamch, and K. cA. Wilk, Colloids Surf., A **442**, 42 (2014).

[40]K. Kassab, J. Photochem. Photobiol. B **68**, 15 (2002).

[41]U. Bazylińska, J. Kulbacka, and K. A. Wilk, Colloids Surf., A **460**, 312 (2014).

[42]E. Jedrych, Z. Pawlicka, M. Chudy, A. Dybko, and Z. Brzozka, Anal. Chim. Acta **683**, 149 (2011).

[43]F. Cuomo, F. Lopez, and A. Cegle, Adv. Colloid Interface Sci. **205**, 124 (2014).

[44]S. Barua and S. Mitragotri, Nano Today **9**, 223 (2014).

[45]See supplementary material at http://dx.doi.org/10.1063/1.4941681 for (1) UV–Vis absorption spectra and a picture of empty and IR-780-loaded nanocapsules 1 and cyanine IR-780 dissolved in acetone:water (1:1) mixture, (2) photooxidation of human serum albumin (0.8 mg/ml) upon irradiation in the presence of native and encapsulated in nanocapsules 2 IR-780 cyanine, (3) *in vitro* release profiles of IR-780 from multilayer nanocapsules in the presence and absence of HSA for synthesized nanocapsules, (4) intracellular distribution of nanocapsules 1 and 2 in A549 and MRC-5 cells, (5) images of MRC-5 and A549 cells after PDT procedures, and (6) photooxidation rate constants (k_v) of HSA sensitized by the free end encapsulated IR-780 cyanine at different concentrations.

[46]B. Zhao, J. J. Yin, P. J. Bilski, C. F. Chignell, J. E. Roberts, and Y. Y. He, Toxicol. Appl. Pharmacol. **241**, 163 (2009).

[47]L. S. Murakami, L. P. Ferreira, J. S. Santos, R. S. da Silva, A. Nomizo, V. A. Kuzmin, and I. E. Borissevitch, Biochim. Biophys. Acta **1850**, 1150 (2015).